

Perturbative operator approach to high-precision light-pulse atom interferometryChristian Ufrecht^{✉*} and Enno Giese[✉]*Institut für Quantenphysik and Center for Integrated Quantum Science and Technology (IQST), Universität Ulm, Albert-Einstein-Allee 11, D-89069 Ulm, Germany*

(Received 4 March 2020; accepted 15 April 2020; published 8 May 2020)

Light-pulse atom interferometers are powerful quantum sensors, however, their accuracy for example in tests of the weak equivalence principle is limited by various spurious influences like stray magnetic fields or blackbody radiation. Improving the accuracy therefore requires a detailed assessment of the size of such deleterious effects. Here we present a systematic operator expansion to obtain phase shift and contrast analytically in powers of a perturbation potential. The result can either be employed for robust straightforward order-of-magnitude estimates or for rigorous calculations. Together with general conditions for the validity of the approach, we provide a particularly useful formula for the phase including wave-packet effects.

DOI: [10.1103/PhysRevA.101.053615](https://doi.org/10.1103/PhysRevA.101.053615)**I. INTRODUCTION**

Since their first implementation [1] in 1991 the accuracy of light-pulse atom interferometers has been improved considerably, which led to high-precision applications in gravimetry [2,3], gradiometry [4–6], tests of fundamental physics such as the weak equivalence principle [7–10], measurements of the fine-structure constant [11,12], and proposals for gravitational-wave detection [13]. However, as the accuracy is pushed further, an increasing number of formerly negligible influences such as magnetic field gradients, blackbody radiation inducing a spatially dependent ac Stark shift [14,15], or gravitational fields of the laboratory environment have to be included into the error budget. In this article we present a systematic approach to account for such spurious effects.

Although phase shifts caused by the corresponding in general anharmonic potential shifts can be small, they might nevertheless be non-negligible which calls for a systematic perturbative approach. Over the years, several powerful analytic methods for the calculation of phase and contrast of light-pulse atom interferometers have been developed based on the Feynman path integral [16,17], descriptions in phase space [18,19], as well as in the form of representation-free descriptions on the operator level for linear gravity [20], path-independent quadratic Hamiltonians [21,22], or within a local-harmonic [23,24] approximation. Within the latter approach, it was also possible to obtain wave-packet effects to lowest order [25]. However, these methods are either applicable to at most quadratic potentials or lack a comprehensive discussion of consistency in the case of more general applications.

In this article we derive a systematic perturbative description for phase and contrast including effects due to wave-packet dynamics based on two formal series, the Magnus [26–29] and the cumulant [30] expansion. They have already been applied in the context of light-pulse atom interferometry

[28] to determine the quality of magnetic shielding [31] and to calculate relativistic effects for interferometric redshift tests [32]. Recently, the Magnus expansion was furthermore used to take into account the effect of finite pulse duration [33]. In this article we extend the work of Ref. [28] with particular emphasis on general conditions for the validity of the approach, characterizing the magnitude of the perturbations.

In Sec. II we outline our main results and put them into context. Subsequently, in Sec. III we introduce our path-dependent model and derive the perturbative expansion. The conditions under which our method is valid will be discussed in Sec. IV. Finally in Sec. V, as a simple example, we apply the formalism to the cubic potential appearing in the Taylor expansion of the gravitational potential of Earth.

II. BRANCH-DEPENDENT DESCRIPTION

Light-pulse atom interferometers consist of a sequence of light pulses which coherently split the initial wave packet and subsequently direct the atoms along the two branches of the interferometer. After recombination by a final laser pulse, the number of atoms at each exit port displays an interference pattern from which the relative phase accumulated between the branches of the interferometer can be inferred. In this work we assume that the Hamiltonian describing the motion through the interferometer can be decomposed into a dominant part (linear gravity, laser pulses) and a weak perturbation (e.g., gravity gradients, blackbody radiation, etc.). As illustrated by the Mach-Zehnder (MZ) gravimeter shown in Fig. 1, the two branches of the interferometer are mainly caused by the dominant part of the Hamiltonian (thick solid lines in the figure). These trajectories are only slightly disturbed by the perturbation potentials (leading to the thin dashed lines in the figure), which can in general be different for each branch and time dependent. The hypothetical interferometer sequence with vanishing perturbation will be referred to in the following as *unperturbed interferometer*.

Neglecting wave-packet effects, it has been shown [16,23,25,28] that the phase ϕ of such an interferometer can

*christian.ufrecht@gmx.de

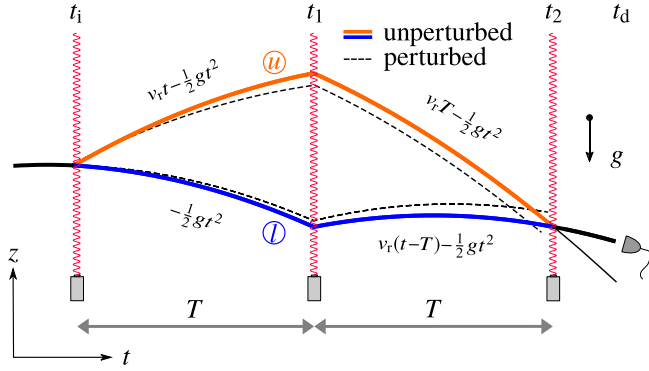


FIG. 1. Mach-Zehnder gravimeter. Initially released from an atomic trap, the free fall of the atoms is interrupted by a $\pi/2$ pulse at $t = t_i = 0$ to split the wave packet into two components transferring a momentum of $\hbar k$ to one of them, which gains the recoil velocity $v_r = \hbar k/m$. After a time T both components are redirected by a π pulse at $t_1 = T$ and finally recombined by a second $\pi/2$ pulse at $t_2 = 2T$. At the detection time t_d the number of particles is measured at one of the exit ports, which forms an interference pattern dependent on the relative phase accumulated between the two branches. The unperturbed branches (thick solid lines) are determined by the analytic expressions shown next to them, where g is the local gravitation acceleration. The perturbation $V^{(\alpha)}$ slightly disturbs the atoms, leading to the deviating branches of the actual interferometer (thin dashed lines).

be obtained from the classical trajectories through

$$\phi = \Delta S/\hbar + \phi_s, \quad (1)$$

where $\Delta S = S^{(u)} - S^{(l)}$ is the classical action difference between the upper and lower branch (superscripts u and l) in combination with a separation phase ϕ_s in case the classical trajectories do not coincide upon detection. In this case we refer to the interferometer as *open*. The calculation of the phase via Eq. (1) therefore consists of (i) solving the differential equation for the classical trajectories including all perturbations and (ii) evaluating the action difference. In the case of weak perturbing potentials, however, this approach is unfavorable for the following reasons: In general, analytic expressions for the trajectories including the perturbation do not exist. Therefore, the trajectories can be solved iteratively to desired order in the perturbation [23] and are then substituted into Eq. (1), possibly resulting in cumbersome expressions, whereas a direct perturbative expansion in powers of the weak perturbing potential would be much more convenient. Furthermore, if the perturbation is only available numerically, in an integration of Eq. (1) one has to account for both the dominant contribution as well as the perturbation, which can be difficult numerically since they likely differ in size by multiple orders of magnitude. Finally, the validity of Eq. (1) is premised on negligible wave-packet effects. However, in the presence of anharmonic perturbation potentials the two components of the wave packet will experience different local expansion dynamics along the branches, leading to a slight mismatch and therefore resulting in additional phase contributions upon detection. Consequently, it is *a priori* not obvious if these phases are negligible compared to those of Eq. (1) originating from the perturbation. The approach presented in this article

is based on a systematic operator expansion derived from a full quantum-mechanical description of the interferometer to overcome these problems. It allows formulating conditions for its validity determining exactly when wave-packet effects are negligible or, in turn, calculating their value to desired accuracy.

Denoting the perturbation potential on the upper and lower branch by $V^{(u)}$ and $V^{(l)}$, respectively, we will find for a closed unperturbed interferometer sequence

$$\phi = \phi_0 - \frac{1}{\hbar} \oint dt V(t) - \frac{1}{2\hbar} \oint dt V_{ij}(t) \langle \hat{r}_i(t) \hat{r}_j(t) \rangle \quad (2)$$

for the phase including the leading-order phase shifts from the perturbation, where repeated indices are summed over. In Eq. (2) we defined ϕ_0 as the phase of the unperturbed interferometer which can be calculated for example with the general formula provided in Ref. [34]. The perturbation potential $V(t) = V^{(\alpha)}(\mathbf{r}_0^{(\alpha)}(t))$ might be different on the upper ($\alpha = u$) and lower branch ($\alpha = l$) and is evaluated at the *unperturbed trajectories* $\mathbf{r}_0^{(\alpha)}(t)$. The integrals run from the initial time t_i , where the atoms are released from the trap, up to the detection time t_d on the upper branch and return along the lower branch back to t_i . We stress that the perturbation potential and its second derivative $V_{ij} = \partial_i \partial_j V$ are evaluated at the two unperturbed trajectories, which obviates the solution of a possibly involved differential equation. The initial conditions for the trajectories are $\mathbf{r}_0(t_i) = \langle \hat{\mathbf{r}} \rangle$ and $\dot{\mathbf{r}}_0(t_i) = \langle \hat{\mathbf{p}} \rangle/m$, where the expectation value is taken with respect to the initial wave packet. In Eq. (2) we furthermore defined the operator describing the free evolution of the wave packet

$$\hat{\mathbf{r}}(t) = \hat{\mathbf{r}} - \langle \hat{\mathbf{r}} \rangle + \frac{\hat{\mathbf{p}} - \langle \hat{\mathbf{p}} \rangle}{m} t. \quad (3)$$

Consequently, $\langle \hat{r}_i(t) \hat{r}_j(t) \rangle$, where the indices label the component of the vectors, provides a measure for the width of the wave packet for vanishing perturbation as detailed further below. Solving the classical trajectories and the integral in Eq. (1) to first order in the perturbation, the first two contributions to Eq. (2) can also be derived [35] directly from Eq. (1). The third contribution, however, describes wave-packet effects which are not taken into account by Eq. (1). In neutron interferometry small perturbations can also be taken into account to first order in a WKB-like treatment [36].

III. PERTURBATIVE TREATMENT

We now derive Eq. (2) from a full quantum-mechanical description. In order to calculate the phase measured by a light-pulse atom interferometer, one has to start from the multilevel Hamiltonian including the virtual states necessary for the diffraction process. However, after adiabatic elimination of the auxiliary states [37,38], neglecting atom-atom interactions, and assuming infinitely short laser pulses, the evolution can be reduced to a branch-dependent description [20,28] in which the phase ϕ and contrast C of the interferometer after projection on one exit port is defined by the expectation value of the *overlap operator*

$$\langle \hat{U}^{(l)\dagger} \hat{U}^{(u)} \rangle = C e^{i\phi}, \quad (4)$$

with respect to the initial wave function, where $\hat{U}^{(\alpha)}$ generates the time evolution along branch α . In this article we assume that the Hamiltonian for each branch allows the decomposition

$$\hat{H}^{(\alpha)} = \hat{H}_0^{(\alpha)} + V^{(\alpha)}(\hat{\mathbf{r}}, t). \quad (5)$$

The perturbation potential $V^{(\alpha)}(\hat{\mathbf{r}}, t)$ only slightly disturbs the dominant part of the evolution which is caused by the unperturbed Hamiltonian

$$\hat{H}_0^{(\alpha)} = \frac{\hat{\mathbf{p}}^2}{2m} + mg\hat{z} + V_{\text{em}}^{(\alpha)}(\hat{\mathbf{r}}, t) \quad (6)$$

describing the motion of an atom with mass m in the linear gravitational field, where g is the local gravitational acceleration. The interaction with the laser pulses is modeled by the potentials

$$V_{\text{em}}^{(\alpha)}(\hat{\mathbf{r}}, t) = -\hbar \sum_{\ell} [\mathbf{k}_{\ell}^{(\alpha)} \hat{\mathbf{r}} + \varphi_{\ell}^{(\alpha)}] \delta(t - t_{\ell}), \quad (7)$$

which transfer the momentum $\hbar \mathbf{k}_{\ell}^{(\alpha)}$ on branch α at time $t = t_{\ell}$ and imprint the laser phase $\varphi_{\ell}^{(\alpha)}$ evaluated at the time of the pulse on the wave packet. In this article we assume that the unperturbed interferometer is closed, translating into the condition

$$\hat{U}_0^{(l)\dagger} \hat{U}_0^{(u)} = e^{i\phi_0}, \quad (8)$$

where $\hat{U}_0^{(\alpha)}$ is the time-evolution operator with respect to Eq. (6). The phase of the unperturbed interferometer ϕ_0 is merely a c -number, implying perfect wave-packet overlap at the end of the unperturbed interferometer sequence. However, the interferometer including the perturbation is in general not closed.

The time-evolution operator with respect to Hamiltonian (5) can be decomposed into

$$\hat{U}^{(\alpha)} = \hat{U}_0^{(\alpha)} \hat{U}_1^{(\alpha)} \quad (9)$$

by transforming into the interaction picture with respect to $\hat{H}_0^{(\alpha)}$ so that the operator

$$\hat{U}_1^{(\alpha)} = \mathcal{T} \exp \left\{ -\frac{i}{\hbar} \int_{t_i}^{t_d} dt \hat{V}_1^{(\alpha)}(t) \right\} \quad (10)$$

only includes the potential $\hat{V}_1^{(\alpha)}(t) = V^{(\alpha)}[\hat{\mathbf{r}}^{(\alpha)}(t), t]$ which is a function of $\hat{\mathbf{r}}^{(\alpha)}(t) = \hat{U}_0^{(\alpha)\dagger} \hat{\mathbf{r}} \hat{U}_0^{(\alpha)}$, the solution of the Heisenberg equations of motion generated by $\hat{H}_0^{(\alpha)}$. An explicit expression for the solution is straightforwardly obtained for our form of $\hat{H}_0^{(\alpha)}$, resulting in $\hat{\mathbf{r}}^{(\alpha)}(t) = \hat{\mathbf{r}} + \hat{\mathbf{p}}t/m + \tilde{\mathbf{r}}_0^{(\alpha)}(t)$. Here $\tilde{\mathbf{r}}_0^{(\alpha)}(t)$ are the classical trajectories caused by the unperturbed Hamiltonian (6) with the initial conditions $\tilde{\mathbf{r}}_0^{(\alpha)}(t_i) = 0$ and $\dot{\tilde{\mathbf{r}}}_0^{(\alpha)}(t_i) = 0$ since the Schrödinger and Heisenberg picture coincide at $t = t_i$.

Inserting the decomposition shown in Eq. (9) into the overlap operator in Eq. (4) then yields

$$\hat{U}^{(l)\dagger} \hat{U}^{(u)} = \hat{U}_1^{(l)\dagger} \hat{U}_0^{(l)\dagger} \hat{U}_0^{(u)} \hat{U}_1^{(u)} = e^{i\phi_0} \hat{U}_1^{(l)\dagger} \hat{U}_1^{(u)}. \quad (11)$$

Recalling Eq. (8), we identified the phase of the closed unperturbed interferometer and moved the exponential $\exp(i\phi_0)$ to

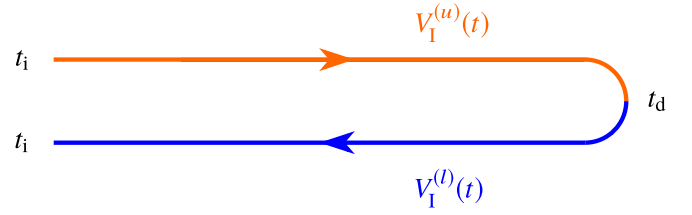


FIG. 2. Time contour. To merge the two time-evolution operators corresponding to the two branches of the interferometer, we introduce the time contour depicted in the figure over which all integrals extend. Starting at t_i the integrals run to the detection time t_d over the perturbation potential corresponding to the upper branch and subsequently return along the lower branch back to the initial time t_i .

the left as it is only a c -number. Writing the two interaction picture time-evolution operators explicitly

$$\hat{U}_1^{(l)\dagger} \hat{U}_1^{(u)} = \overline{\mathcal{T}} \exp \left\{ \frac{i}{\hbar} \int_{t_i}^{t_d} dt \hat{V}_1^{(l)} \right\} \mathcal{T} \exp \left\{ -\frac{i}{\hbar} \int_{t_i}^{t_d} dt \hat{V}_1^{(u)} \right\}, \quad (12)$$

we note that the time-ordering operator \mathcal{T} orders times (reading from right to the left) from the initial time t_i to the final time t_d while the anti-time-ordering operator $\overline{\mathcal{T}}$ orders from t_d back to t_i . Thus, we merge the two time-evolution operators to one path-ordered exponential by introducing the path-ordering operator \mathcal{T}_p so that we obtain

$$\hat{U}^{(l)\dagger} \hat{U}^{(u)} = e^{i\phi_0} \mathcal{T}_p \exp \left\{ -\frac{i}{\hbar} \oint dt \hat{V}_1(t) \right\}. \quad (13)$$

Resorting to the concept of path ordering, initially introduced by Schwinger and Keldysh [39,40] in the context of thermal field theory, \mathcal{T}_p orders time along the contour illustrated in Fig. 2. On this contour we define $\hat{V}_1(t) = \hat{V}_1^{(u)}(t)$ for t on the upper path and $\hat{V}_1(t) = \hat{V}_1^{(l)}(t)$ for t on the lower path. With these definitions in mind, we disregard the explicit labeling (α) of the branch if not necessary.

In order to associate the operator $\hat{\mathbf{r}}(t)$ with the unperturbed trajectory of the atoms, the initial mean momentum and position can be included by introducing $\mathbf{r}_0(t) = \tilde{\mathbf{r}}_0(t) + \langle \hat{\mathbf{r}} \rangle + \langle \hat{\mathbf{p}} \rangle t/m$ so that

$$\hat{\mathbf{r}}(t) = \mathbf{r}_0(t) + \hat{\tilde{\mathbf{r}}}(t) \quad (14)$$

for each branch, where $\hat{\tilde{\mathbf{r}}}(t)$ was defined in Eq. (3). Consequently, with Eq. (13) the overlap operator can be written as a path-ordered exponential in which the perturbation potential is evaluated at the classical unperturbed trajectory plus an operator part with vanishing expectation value. The expectation value $\langle \hat{\tilde{\mathbf{r}}}_j(t)^2 \rangle = \Delta r_j^2 + \Delta p_j^2 t^2/m^2$, where Δr_j , Δp_j are the initial position and momentum widths of the wave packet in the j th direction, is therefore a measure for the width of the expanding wave packet as long as any distortion effects from the perturbation potential are negligible. Note that we disregarded for the moment possible initial correlations between $\hat{\mathbf{r}}$ and $\hat{\mathbf{p}}$. Thus, if the change of the potential over the size of the wave packet on each interferometer branch is sufficiently small, the Taylor expansion around the classical trajectory

$\mathbf{r}_0(t)$,

$$\hat{V}_1(t) = V + V_i \hat{r}_i + \frac{1}{2} V_{ij} \hat{r}_i \hat{r}_j + \dots, \quad (15)$$

where indices of the potential again denote derivatives, accurately approximates the potential by taking into account only a few terms. Note that we omitted the time dependence on the right-hand side for the sake of readability and again use the summation convention.

The overlap operator from Eq. (13) still contains the formal path-ordering operator \mathcal{T}_p , prohibiting any further manipulation of the contour-ordered exponential. To remove the former, we apply the Magnus expansion, detailed in Appendix A, facilitating an exponential representation of a time-ordered exponential in terms of a formal series, namely

$$\hat{U}^{(l)\dagger} \hat{U}^{(u)} = e^{i\phi_0 + i\hat{\phi}} = \exp \left\{ i \sum_{n=0}^{\infty} \hat{\phi}_n \right\}, \quad (16)$$

where $\hat{\phi} = \sum_{n=1}^{\infty} \hat{\phi}_n$. For a more convenient notation, the operator $\hat{\phi}_0$ is in fact defined as the phase of the unperturbed interferometer ϕ_0 , i.e., a c -number. The other contributions $\hat{\phi}_n$ for $n > 0$ are determined by the Magnus expansion. In Appendix A we provide the terms explicitly to third order; and in general $\hat{\phi}_n$ contains n nested integrals along the time contour over nested commutators of order $n - 1$ between the potential evaluated at different times.

The Magnus expansion therefore leads to an operator expansion in powers of the perturbation potential V . If small as defined in the following section, the Magnus expansion can be truncated at desired order and we have already succeeded in finding an approximate exponential representation of the overlap operator. However, according to Eq. (4), it is still necessary to evaluate the expectation value of this operator. In case of a path-independent harmonic potential it can be shown [22] that the exponent of the overlap operator depends only linearly on $\hat{\mathbf{r}}$ and $\hat{\mathbf{p}}$, making the calculation of the expectation value straightforward. However, in general such a simple representation does not exist and the overlap operator will contain various powers of $\hat{\mathbf{r}}$ and $\hat{\mathbf{p}}$. In this case, a suitable approach lies in the cumulant expansion, a formal series, casting the expectation value of an exponential operator into the form

$$\langle e^{i\hat{\phi}} \rangle = \exp \left\{ \sum_{n=1}^{\infty} \frac{\kappa_n}{n!} \right\}, \quad (17)$$

where the cumulants κ_n , defined in Appendix B, are functions of the first n moments of $\hat{\phi}$. Consequently, the phase of an interferometer can at least formally be expressed in powers of the perturbation potential.

Truncating the series at some desired order, however, requires a detailed assessment of conditions characterizing the magnitude of the potential and the size of wave-packet effects. These conditions for the validity of our approach will be discussed in the subsequent section.

For the moment let us assume that these conditions are satisfied, allowing a truncation of the Magnus and cumulant expansion at first order. Consequently, with the help of Eqs. (16) and (B6) the phase is $\phi = \phi_0 + \langle \hat{\phi}_1 \rangle$. Inserting the Taylor polynomial of the potential up to quadratic order into

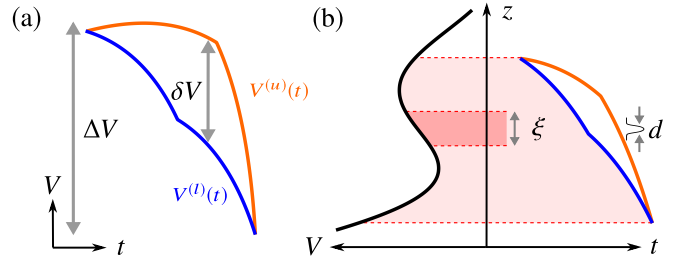


FIG. 3. Comparison between different scales. (a) Perturbation potential evaluated at the two unperturbed trajectories spanning the interferometer as a function of time (blue and orange curve). Whereas ΔV corresponds to the maximal potential difference probed by the atoms, δV is the maximal potential difference between the branches of the interferometer, which is generally smaller. (b) The space-time diagram of a given interferometer sequence determines the domain of the potential probed by the atoms (colored in bright red). The suppression factor of consecutive terms in the Magnus expansion as well as wave-packet effects are crucially dependent on the value of ξ which is the length scale on which the potential changes. If we assign a wave number to the oscillatory behavior of the potential shown in the figure, ξ is given by its inverse (colored in darker red). In contrast, in the case of a simple polynomial form of the potential, the value of ξ would scale with the extent of the interferometer itself. A third length scale is determined by the characteristic size of the wave-packet d .

Eq. (A2) and recalling that $\langle \hat{\mathbf{r}} \rangle = 0$, we arrive at Eq. (2), the main result of our article.

IV. CONDITIONS FOR VALIDITY

We now derive conditions for the validity of the perturbative treatment presented in the section above. First, we introduce a characteristic length scale ξ with

$$\Delta V \sim \xi^n \Delta V^{(n)}, \quad (18)$$

where ΔV is the difference between the extremal values of the potential probed by the atoms over the course of the interferometer. Furthermore, $\Delta V^{(n)}$ is the typical value of the n th derivative of the potential. For example, in case of a power-law dependence of the potential, ξ corresponds to the size of the atomic fountain in which the experiment is performed while for oscillating potentials the value of ξ can be much smaller. The parameters ΔV and ξ are visualized in Fig. 3 together with further quantities defined below.

First, a perturbative treatment is only valid, if the deviation of the unperturbed trajectories caused by the perturbation potential is small compared to the characteristic length scale ξ on which the potential varies. Therefore, identifying an acceleration $a \sim -\Delta V/(m\xi)$ of the atom due to the perturbation potential, where $\Delta V/\xi \sim \Delta V^{(1)}$, we require that the distance aT^2 is much smaller than the characteristic length ξ , that is

$$\epsilon = \frac{\Delta VT^2}{\xi^2 m} \ll 1, \quad (19)$$

where T denotes the characteristic interferometer time which can be chosen to be equal to the interrogation time of the interferometer. As shown more rigorously in Appendix D, the

TABLE I. Explicit values for ξ , ϵ , d/ξ , and $\eta d/\xi$ for different sources of the perturbation. In the table we show that all these examples satisfy the conditions for the validity of our approach. The parameters ΔV , δV , and ξ used for the calculation of ϵ and η are estimated from the potentials stated in the references. The width of the wave packet is assumed to be $d = 50 \mu\text{m}$.

	Gravity gradients [41]	Magnetic field gradients [31]	Blackbody radiation [15]	Mass defect in quantum clocks [32]
ξ (m)	0.1	0.1	0.01	10
ϵ	10^{-8}	10^{-11}	10^{-5}	10^{-12}
d/ξ	5×10^{-4}	5×10^{-4}	5×10^{-3}	5×10^{-6}
$\eta d/\xi$	10^{-4}	10^{-9}	10^{-3}	10^{-9}

parameter ϵ constitutes the factor by which subsequent orders of the Magnus expansion are suppressed.

We now consider the leading-order correction to the unperturbed phase, which is the second term on the right-hand side of Eq. (2). This term can be estimated to be of the size

$$\eta = \frac{\delta VT}{\hbar}, \quad (20)$$

where δV is the maximal potential difference between the branches at one instance of time, which can be much smaller than ΔV , the difference between the two extremal values of the potential probed by the atoms during the course of the interferometer.

In Eq. (15) we Taylor expanded the potential about the unperturbed trajectory over the size of the wave packet represented by the operator \hat{r} . Heuristically replacing the position operators by the wave-packet width d , the Taylor expansion can be truncated after a few terms if $\Delta V^{(n)} d^n \ll \Delta V$ which translates with the help of Eq. (18) into

$$d/\xi \ll 1. \quad (21)$$

Finally, if this condition holds, the *leading-order* operator-valued term in $\hat{\phi}$ is due to the *first-order* term in the Taylor expansion of the potential, taking the form $\int dt V_i \hat{r}_i / \hbar$. To guarantee the validity of the cumulant expansion, which is a function of the moments of $\hat{\phi}$, this term should be much smaller than unity. This requirement can be expressed by

$$\eta d/\xi \ll 1 \quad (22)$$

after again replacing the operator \hat{r} by d , the integration in time by the characteristic interferometer time T , and by making use of Eq. (18). A more rigorous derivation of these conditions can be found in Appendix D.

In Table I we give approximate values for ξ , ϵ , and $\eta d/\xi$ for some experiments or recent proposals. As shown in the table, the accuracy achieved by truncation of the Magnus expansion at first order often is already sufficient and our formalism is well suited to be applied to these situations.

Obviously a scaling such as in Eq. (18) cannot be guaranteed in general. For this case we apply the Magnus expansion to the Taylor polynomial of the perturbation potential explicitly in Appendix C from which the scaling of phase shifts can be inferred. However, for many applications a parameter ξ does exist, satisfying Eq. (18) at least approximately, which is sufficient for an order-of-magnitude estimation of the size of phase shifts beyond Eq. (2).

V. EXAMPLE: GRAVITATIONAL POTENTIAL

In this section we illustrate the formalism derived in the previous sections by the example of an MZ-interferometry experiment conducted in the Newtonian gravitational potential of Earth

$$V(\mathbf{r}) = -G \frac{mM}{r}, \quad (23)$$

where G is Newton's constant and M is the mass of Earth. Choosing the z axis of a new coordinate system in direction of Earth's radius R , we Taylor expand the potential around a point on Earth's surface in powers of R^{-1} . This calculation yields

$$V(\mathbf{r}) = mgz + \frac{1}{2} m \Gamma_{ij}^{(1)} r_i r_j + \frac{1}{6} m \Gamma_{ijl}^{(2)} r_i r_j r_l + O(R^{-3}) \quad (24)$$

after omitting the irrelevant constant. The only nonvanishing components of the fully symmetric first and second gravity-gradient tensors $\Gamma^{(1)}$ and $\Gamma^{(2)}$ then are given by

$$\Gamma_{xx}^{(1)} = \Gamma_{yy}^{(1)} = \frac{g}{R}, \quad \Gamma_{zz}^{(1)} = -2 \frac{g}{R}, \quad (25)$$

and (including all possible permutations)

$$\Gamma_{xxz}^{(2)} = \Gamma_{yyz}^{(2)} = -3 \frac{g}{R^2}, \quad \Gamma_{zzz}^{(2)} = 6 \frac{g}{R^2}, \quad (26)$$

where we identified $g = GM/R^2$. Phase corrections caused by the first gradients (described by $\Gamma^{(1)}$) have been calculated to all orders in $\Gamma^{(1)}$ [22,42]. However, note that phase contributions to second order in $\Gamma^{(1)}$ and to first order in $\Gamma^{(2)}$ both scale with R^{-2} and may therefore be of the same size, making the calculation inconsistent when disregarding $\Gamma^{(2)}$.

In this example we focus on the second gravity gradients (described by $\Gamma^{(2)}$). Phase shifts from this contribution have been calculated before [23] but here we will additionally include the contribution of wave-packet effects. Furthermore, we stress how straightforward the calculation becomes with our formalism and put particular emphasis on the application of the conditions for the validity of a perturbative description.

A. Check of conditions for validity

First we check condition (19) for the validity of the Magnus expansion. Because of the polynomial form of the potential, ξ is given by the total extent of the interferometer. Assuming the recoil velocity $v_r = \hbar k/m$, where $\hbar k$ is the effective momentum transfer of the lasers as well as the initial velocity of the atoms v_i to be much smaller than gT , the size of the interferometer scales with $\xi = gT^2/2$ and we choose $\Delta V = m \Gamma^{(2)} \xi^3$, where T is half of the interferometer time (see

Fig. 1). Consequently, with the help of Eq. (19),

$$\epsilon = \Gamma^{(2)} g T^4 \approx 10^{-12} \quad (27)$$

for $T \approx 1$ s. Consecutive terms in the Magnus expansion corresponding to the same power of the operators \hat{r} and \hat{p} are therefore suppressed by this factor and a consideration to first order is sufficient. Next we calculate the potential difference between the interferometer branches by inserting the analytic expressions for the unperturbed trajectories from Fig. 1 into the potential so that

$$\delta V \sim m \Gamma^{(2)} [(v_r T - g T^2/2)^3 - (-g T^2/2)^3] \sim m \Gamma^{(2)} g^2 v_r T^5, \quad (28)$$

where we replaced $t \sim T$. Consequently, the leading-order phase shift from the second gravity gradients is of the order of

$$\eta = \Gamma^{(2)} \frac{m g^2 v_r T^6}{\hbar} = \Gamma^{(2)} k g^2 T^6 \approx 10^{-4}, \quad (29)$$

where, as the momentum transfer stems from a two-photon process, the value $k = 4\pi/(780 \text{ nm})$ of the effective wave number corresponds to twice the wave length of the D_2 line of rubidium 87.

Finally, it is left to examine condition (22) for the validity of the cumulant expansion. Note that in principle one should consider operator-valued contributions in the overlap operator from the first *and* second gravity gradients but for the sake of a simple presentation we restrict the discussion to latter. Assuming a maximal size $d = 200 \mu\text{m}$ of the wave packet, we find

$$\eta d / \xi \approx 10^{-9} \quad (30)$$

so that Eq. (2) can be confidently applied.

B. Calculation of phase

We now consider a general interferometer sequence, but for simplicity we assume the laser pulses to be aligned with the direction of linear gravity so that the classical unperturbed trajectories take the form $r_{0j}(t) = z_0(t) \delta_{zj}$. Insertion of the perturbing potential into Eq. (2) then yields for the phase shift due to $\Gamma^{(2)}$,

$$\frac{1}{\hbar} \oint dt V(t) = \frac{m}{6\hbar} \Gamma_{zzz}^{(2)} f_\phi \quad (31)$$

and

$$\begin{aligned} & \frac{1}{2\hbar} \oint dt V_{ij}(t) \langle \hat{r}_i(t) \hat{r}_j(t) \rangle \\ &= \frac{1}{2\hbar} \Gamma_{zij}^{(2)} \left[m \langle \hat{r}_i \hat{r}_j \rangle_c f_{rr} + \langle \hat{r}_i \hat{p}_j + \hat{p}_j \hat{r}_i \rangle_c f_{rp} + \frac{1}{m} \langle \hat{p}_i \hat{p}_j \rangle_c f_{pp} \right], \end{aligned} \quad (32)$$

where we recalled Eq. (3) and defined the *central expectation value* $\langle \cdot \rangle_c$ with respect to the initial state but displaced by $\langle \hat{r} \rangle$ and $\langle \hat{p} \rangle$ to the origin of phase space so that, e.g., $\langle \hat{r}_i \hat{r}_j \rangle_c = \langle (\hat{r}_i - \langle \hat{r}_i \rangle) (\hat{r}_j - \langle \hat{r}_j \rangle) \rangle$. In Eqs. (31) and (32) we made furthermore use of the symmetry of $\Gamma^{(2)}$. The chosen interferometer sequence only enters the expression through the functions f_ϕ , f_{rr} , f_{rp} , and f_{pp} defined in Appendix E and also explicitly

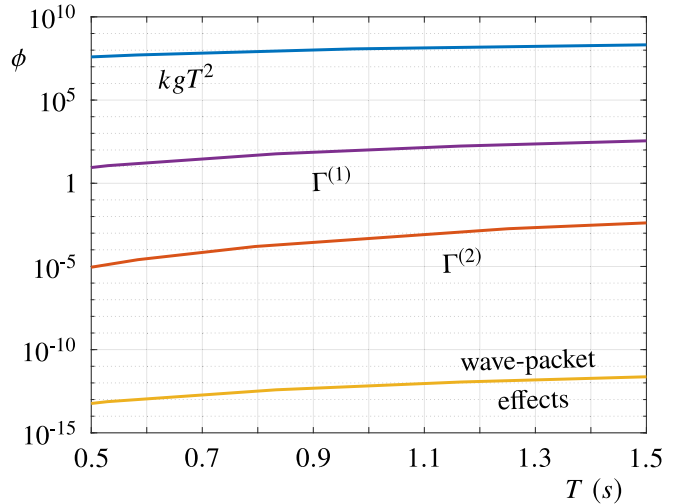


FIG. 4. Plot of phase shifts caused by the gravitational field of Earth. As shown in the figure, the dominant contribution kgT^2 to the phase (blue line) is due to the unperturbed interferometer. The phase shift caused by the first gravity gradients [41] scales with R^{-1} (purple line). Phase contributions from the second gravity gradients scale with R^{-2} and can be divided into the first term inside the bracket in Eq. (33) (orange line) and the second term which originates from wave-packet effects (yellow line). For this figure the parameters are: The radius of Earth is $R \simeq 6 \times 10^6$ m, the effective wave vector is given by $k = 4\pi/(780 \text{ nm})$, an interferometer time of $T = 1$ s is assumed, the initial trapping frequency is $\omega = 2\pi \times 60$ Hz, and a mass corresponding to rubidium 87 is chosen.

evaluated for the MZ geometry depicted in Fig. 1. In order to keep the expressions compact, we assume the initial position $r_{0j}(t_i) = z_i \delta_{jz}$ without an initial velocity. If necessary, however, a more general calculation is straightforward. As shown in Appendix E, the phase then depends on the initial position z_i of the state. This result is a direct consequence of the operator-valued form of the overlap operator. In contrast, if the interferometer is closed, the overlap operator reduces to a c -number and its expectation value is independent of the wave function and therefore of the initial conditions.

To obtain compact explicit expressions for the phase shift due to wave-packet effects, we assume that the first laser pulse acts right after releasing the atoms from the trap. Thus, assuming the initial state as the ground state of a harmonic trap with frequency ω_i in the i th direction results in $\langle \hat{r}_i \hat{r}_j \rangle_c = \delta_{ij} \hbar / (2m\omega_i)$ and $\langle \hat{p}_i \hat{p}_j \rangle_c = \delta_{ij} \hbar m \omega_i / 2$ as well as vanishing correlations between momentum and position operators. Specifying further $\omega \equiv \omega_x = \omega_y = 2\omega_z$, the final result for the lowest-order correction due to the cubic potential is

$$\phi = \phi_0 - \frac{g}{R^2} \left[\frac{m}{\hbar} f_\phi + \frac{v_r T^2}{\omega} \left(\frac{3}{2} - \frac{7}{8} (\omega T)^2 \right) \right]. \quad (33)$$

Interestingly, if the atoms expanded out of a symmetric harmonic trap, the wave-packet induced contributions would vanish.

In Fig. 4 we illustrate Eq. (33) for reasonable experimental parameter values. In the figure we compare the phase of the unperturbed interferometer sequence (blue line) and the phase due to $\Gamma^{(1)}$ (purple line) [41] to the phase shift calculated in

Eq. (33) from the cubic contribution of the Taylor expansion (orange line). The effect of phase shifts caused by $\Gamma^{(1)}$ are generally relevant in state-of-the-art precision measurements [41]. As a consequence, such phase contributions either have to be included into the analysis, or have to be compensated through differential schemes [8] (for example used for test of the weak equivalence principle) and mitigation techniques [43]. Phase shifts originating from second gradients $\Gamma^{(2)}$, however, are of the order of magnitude to possibly limit future spaceborne missions if not appropriately accounted for. Finally, the phase shift originating from different expansion dynamics along the branches (yellow line) is beyond any accessible value for light-pulse atom interferometric experiments in the mid future. Such phases, however, can be much larger when taking into account the inhomogeneous gravitational field of the laboratory environment.

VI. DISCUSSION AND CONCLUSION

Obviously Hamiltonian (5) does not account for atom-atom interactions. However, state-of-the-art atom interferometers employ Bose-Einstein condensates as highly coherent atom sources which are intrinsically interacting many-body systems. Nonetheless, numerical propagation of the initial mean-field state with the help of the Gross-Pitaevskii equation, including release from the trap and possibly magnetic lensing [44], shows that due to the dynamical expansion, the strength of interactions quickly decreases. Thus, if the initial expansion time before the first laser pulse is sufficiently large, any further evolution will be accurately described by the Schrödinger equation and our formalism is valid from this instance of time. Then, the state right before the first laser pulse is used as input [24] and the expectation value of the overlap operator is calculated with respect to this state. Even more if interactions are negligible during the whole experiment, we include the time between release and first laser pulse into the unperturbed trajectories so that the influence of the perturbation on the wave packet during this initial expansion time is automatically accounted for. It then suffices to calculate expectations values with respect to the ground state of the trap.

In our article we have restricted the discussion to perturbations which only depend on the position operator \hat{r} . A generalization, however, of our results for the application to \hat{p} -dependent perturbations, present for example in rotating frames, is straightforward.

The application of the Magnus expansion to the overlap operator has resulted in nested contour integrals whose analytical evaluation becomes cumbersome for large orders of the expansion. Even though the integrals can be reordered [28] to streamline analytical calculations, the loop structure of the integral is particularly useful in a numerical implementation. Here the perturbation potential (and its derivatives) are discretized exactly on the time contour so that a numerical integration algorithm will automatically account for the loop properties of the integrals.

Our approach is applicable to a variety of situations with different sources of the perturbation, including, e.g., black-body radiation, gravity gradients, inhomogeneities in the gravitational potential of the laboratory environment, magnetic

field gradients, relativistic effects, violation parameters of the universality of free fall, and finite laser pulse lengths.

In this work we proposed a perturbative tool to assess small phases due to spurious influences for light-pulse atom interferometers. Making use of a path-dependent description formalized by the introduction of the path-ordering operator, we emphasized how the method solves the problems of previous results. Based on two formal series, the Magnus and cumulant expansion, we derived Eq. (2) for the leading-order phase shifts originating from the perturbation including wave-packet effects and obtained detailed conditions for the validity of our approach which are stated in Eqs. (19), (21), and (22). Finally, we commented on straightforward generalizations and the numerical implementation in case analytic calculations are not possible.

ACKNOWLEDGMENTS

We thank F. Di Pumpo, A. Friedrich, A. Roura, and W. P. Schleich for helpful discussions. This work is supported by the German Aerospace Center (Deutsches Zentrum für Luft- und Raumfahrt, DLR) with funds provided by the Federal Ministry for Economic Affairs and Energy (Bundesministerium für Wirtschaft und Energie, BMWi) due to an enactment of the German Bundestag under Grants No. DLR 50WM1556 and No. 50WM1956. We thank the Ministry of Science, Research and Art Baden-Württemberg (Ministerium für Wissenschaft, Forschung und Kunst Baden-Württemberg) for financially supporting the work of IQST.

APPENDIX A: MAGNUS EXPANSION

The Magnus expansion [26–28] is a formal series for the exponential representation of a time-ordered exponential

$$\hat{U} = \mathcal{T} \exp \left\{ -\frac{i}{\hbar} \int_{t_i}^{t_d} dt \hat{H}(t) \right\} = \exp \left\{ i \sum_{n=1}^{\infty} \hat{\phi}_n \right\}, \quad (\text{A1})$$

where $\hat{H}(t)$ is a time-dependent Hamiltonian. Applied to the path-ordered exponential in Eq. (13), we obtain for the first three elements of the series in Eq. (16),

$$\hat{\phi}_1 = -\frac{1}{\hbar} \oint dt \hat{V}_1(t), \quad (\text{A2})$$

$$\hat{\phi}_2 = \frac{i}{2\hbar^2} \oint dt \oint dt' [\hat{V}_1(t), \hat{V}_1(t')], \quad (\text{A3})$$

$$\begin{aligned} \hat{\phi}_3 = & \frac{1}{6\hbar^3} \oint dt \oint dt' \oint dt'' ([\hat{V}_1(t), [\hat{V}_1(t'), \hat{V}_1(t'')]] \\ & + [\hat{V}_1(t''), [\hat{V}_1(t'), \hat{V}_1(t)]]). \end{aligned} \quad (\text{A4})$$

In general, $\hat{\phi}_n$ consists of n nested integrals over $(n-1)$ -th order commutators between the potential evaluated at different times. The perturbation potential is a function of the solution of the Heisenberg equations of motion $\hat{r}(t)$ generated by the unperturbed Hamiltonian.

APPENDIX B: CUMULANT EXPANSION

The cumulant expansion [30,45] is a formal series for an exponential representation of the expectation value of an

exponential operator which is defined by

$$\langle e^{i\hat{\phi}\zeta} \rangle = \exp \left\{ \sum_{n=1}^{\infty} \frac{\kappa_n}{n!} \zeta^n \right\}, \quad (\text{B1})$$

where one introduces a formal expansion parameter ζ , which is set to unity after the calculation, and the coefficients κ_n are referred to as *cumulants*. By taking the logarithm on both sides, we find the definition of the cumulants as

$$\kappa_n = \frac{d^n}{d\zeta^n} \ln \langle e^{i\hat{\phi}\zeta} \rangle |_{\zeta=0}, \quad (\text{B2})$$

where the n th cumulant is function of the first n moments of $\hat{\phi}$. Here we state explicitly the first three cumulants

$$\kappa_1 = i\langle \hat{\phi} \rangle, \quad (\text{B3})$$

$$\kappa_2 = -\langle \hat{\phi}^2 \rangle + \langle \hat{\phi} \rangle^2, \quad (\text{B4})$$

$$\kappa_3 = -i[\langle \hat{\phi}^3 \rangle - 3\langle \hat{\phi}^2 \rangle \langle \hat{\phi} \rangle + 2\langle \hat{\phi} \rangle^3]. \quad (\text{B5})$$

Since $\hat{\phi} = \sum_{n=1}^{\infty} \hat{\phi}_n$ is calculated from the overlap operator by Magnus expansion and is therefore Hermitian, we separate Eq. (B1) into phase and amplitude. By comparing to Eq. (4), we find the phase ϕ of the interferometer

$$\phi = \phi_0 + \langle \hat{\phi} \rangle - \frac{1}{6}[\langle \hat{\phi}^3 \rangle - 3\langle \hat{\phi} \rangle^2 \langle \hat{\phi} \rangle + 2\langle \hat{\phi} \rangle^3] + \dots, \quad (\text{B6})$$

where we included the phase of the unperturbed interferometer ϕ_0 from Eq. (16), and the contrast C is

$$\ln C = -\frac{1}{2}(\langle \hat{\phi}^2 \rangle - \langle \hat{\phi} \rangle^2) + \dots \quad (\text{B7})$$

APPENDIX C: PHASE TO SECOND ORDER

In this Appendix we apply the Magnus expansion to second order to the overlap operator. To this end, we insert the Taylor series of the potential into Eq. (16), where $\hat{\phi}_n$ is determined by the Magnus expansion. Making use of the commutator

$$[\hat{r}_i(t), \hat{r}_j(t')] = \frac{i\hbar}{m}(t' - t)\delta_{ij}, \quad (\text{C1})$$

where δ_{ij} is the Kronecker symbol, we obtain with the help of Eqs. (A2) and (A3)

$$\hat{\phi}_0 = \phi_0, \quad (\text{C2})$$

$$\hat{\phi}_1 = -\frac{1}{\hbar} \oint dt \left\{ V + V_i \hat{r}_i + \frac{1}{2} V_{ij} \hat{r}_i \hat{r}_j + \frac{1}{6} V_{ijk} \hat{r}_i \hat{r}_j \hat{r}_k + \frac{1}{24} V_{ijkl} \hat{r}_i \hat{r}_j \hat{r}_k \hat{r}_l + \dots \right\}, \quad (\text{C3})$$

$$\hat{\phi}_2 = -\frac{1}{2\hbar m} \oint dt \oint dt' (t' - t) \left\{ V_i V'_i + V_i V'_{ij} \hat{r}'_j + V'_i V_{ij} \hat{r}_j + \frac{1}{2} V_{ijk} V'_{ij} \hat{r}'_j \hat{r}_k + \frac{1}{2} V_{ik} V'_{kj} (\hat{r}'_j \hat{r}_i + \hat{r}_i \hat{r}'_j) + \frac{1}{2} V_i V'_{ijk} \hat{r}'_j \hat{r}'_k + \dots \right\}. \quad (\text{C4})$$

Note that all quantities depend on time t or t' . If dependent on the latter, this dependence is abbreviated by a prime on the respective quantity.

APPENDIX D: DERIVATION OF CONDITIONS FOR VALIDITY

In order to complement the validity discussion of Sec. IV, we proceed in two steps. First, we derive the factor ϵ by which subsequent terms in the Magnus expansion are suppressed. Second, we investigate the scaling of different orders in the cumulant expansion.

For the sake of simplicity, in the following we choose one typical direction x and suppress the time dependence of $\hat{x}(t)$ except when appearing in the commutator. Within this simplification we replace the potential and its derivatives in Eq. (15) by their typical size and use Eq. (18) to find $\hat{V}_1 \sim \Delta V \sum_k \hat{x}^k / \xi^k$. With the help of this form of the potential, the commutator becomes

$$[\hat{V}_1(t), \hat{V}_1(t')] \sim \frac{\Delta V^2 \hbar T}{m \xi^2} \sum_k \frac{\hat{x}^k}{\xi^k}, \quad (\text{D1})$$

where we replaced the time difference in Eq. (C1) by the characteristic interferometer time T and suppressed any numerical factors. This result is easily generalized to the $(n-1)$ th order nested commutator (which contains the potential evaluated at n different times) as

$$[\hat{V}_1(t), [\hat{V}_1(t'), [\dots]]]_{n-1} \sim \frac{\Delta V \hbar^{n-1}}{T^{n-1}} \epsilon^{n-1} \sum_k \frac{\hat{x}^k}{\xi^k}, \quad (\text{D2})$$

where ϵ is given in Eq. (19). According to Appendix A the n th-order term $\hat{\phi}_n$ of the Magnus expansion contains $(n-1)$ th-order commutators, a factor $1/\hbar^n$, and n integrals over time which we replace by T^n . Hence, together with Eq. (D2) one again obtains an infinite series

$$\hat{\phi}_n \sim \sum_k c_{kn} \frac{\hat{x}^k}{\xi^k}, \quad (\text{D3})$$

where

$$c_{kn} \sim \frac{\eta \epsilon^{n-1}}{\xi^k} \quad (\text{D4})$$

and η was defined in Eq. (20). Note that, since the final integral in the nested sequence extends along the whole contour, we replaced one factor of ΔV by the maximal potential difference over the separation of the branches δV . Consequently, consecutive terms in the Magnus expansion corresponding to the same power of \hat{x} are suppressed by ϵ independently of the power. Hence, if $\epsilon \ll 1$, the Magnus expansion can be truncated as the prefactors c_{kn} quickly decrease order by order of n .

After performing the Magnus expansion, it remains to calculate the expectation value of the overlap operator. Because this is in general not possible in an exact manner, we resort to the cumulant expansion for which expectation values of powers of \hat{r}_j at different times have to be evaluated. To estimate the size of such expectation values independently of the explicit form of the initial wave function, we truncate the corresponding probability density outside some region with characteristic width d where the probability to find a particle is vanishing. This approximation will allow us to express any moment in terms of the finite width d of the wave function. Note that calculating phase and contrast with the help of the

Magnus and cumulant expansions might lead to divergent series but there will exist a finite number of terms after which truncating the formal series leads to the best approximation in the spirit of an asymptotic expansion.

In order to estimate the expectation value of powers of $\hat{r}_j(t)$, we define the centered wave function $|\psi_c\rangle$, the initial state displaced by $\langle\hat{r}\rangle$ and $\langle\hat{p}\rangle$ to the origin of phase space. Equally, evolving with the free time-evolution operator $\hat{U}(t) = \exp[-i\hat{p}^2 t/(2m\hbar)]$, the freely expanding centered wave function is denoted by $|\psi_c(t)\rangle$. Thus,

$$\begin{aligned} \langle\hat{x}^k(t)\rangle &= \langle\psi_c|(\hat{x} + \hat{p}t/m)|\psi_c\rangle \\ &= \langle\psi_c|\hat{U}^\dagger(t)\hat{x}^k\hat{U}(t)|\psi_c\rangle = \langle\psi_c(t)|\hat{x}^k|\psi_c(t)\rangle \\ &= \int d^3\mathbf{r}|\psi_c(\mathbf{r},t)|^2 x^k = x_d(t)^k \sim d^k. \end{aligned} \quad (\text{D5})$$

First, we removed the expectation values $\langle\hat{r}\rangle$ and $\langle\hat{p}\rangle$ appearing in the definition of $\hat{r}(t)$, see Eq. (3), by calculating the expectation value with respect to centered wave function rather than the actual initial state. In the third line we used the mean-value theorem of integration [46] to find the number $x_d(t)$ within the set where the wave function is nonvanishing, subsequently estimated by the maximal size d of the wave function. Thus, the expectation value of any power of $\hat{x}(t)$ can indeed be expressed in terms of the width d .

However, expectation values of the commutators in the Magnus expansion or higher-order terms of the cumulant expansion involve products between powers of \hat{x} evaluated at different times. The expectation value of such expressions can be calculated for example in Wigner phase space, where one has to take care of the correct operator ordering [47,48]. Nevertheless, the scaling with the size of the wave packet remains similar so that we will, e.g., assume

$$\langle\hat{x}^l(t)\hat{x}^k(t')\rangle \sim d^{l+k}. \quad (\text{D6})$$

With the help of Eqs. (D3) and (D4) we therefore find

$$\langle\hat{\phi}_n\rangle \sim \eta\epsilon^{n-1} \sum_k \left(\frac{d}{\xi}\right)^k \quad (\text{D7})$$

for the expectation value of the n th order of the Magnus expansion.

We now investigate the behavior of the cumulant expansion by considering only the dominant operator-valued term in the overlap operator which is due to $n = 1$ and $k = 1$ in Eq. (D3) provided $\epsilon \ll 1$ and $d/\xi \ll 1$. As explained in Appendix B the l th order of the cumulant expansion is a function of the first l moments which consequently scales as $(\eta d/\xi)^l$ and we therefore require

$$\eta \frac{d}{\xi} \ll 1, \quad (\text{D8})$$

which is condition (22). If satisfied, we also truncate the cumulant expansion at first order and obtain (considering only terms up to harmonic order in the Taylor expansion of the potential) Eq. (2), the main result of this article after recalling $\langle\hat{r}(t)\rangle = 0$.

APPENDIX E: GRAVITATIONAL POTENTIAL

In this Appendix we give the explicit form of the functions f_ϕ , f_{rr} , f_{rp} , and f_{pp} defined in Sec. V to calculate the phase and wave-packet effects arising from $\Gamma^{(2)}$. For an arbitrary pulse sequence encoded in the unperturbed trajectory $z_0(t)$, the coefficients take the form

$$f_\phi = \oint dt z_0(t)^3, \quad f_{rr} = \oint dt z_0(t), \quad (\text{E1})$$

$$f_{rp} = \oint dt z_0(t)t, \quad f_{pp} = \oint dt z_0(t)t^2. \quad (\text{E2})$$

Using the explicit form of $z_0(t)$ for the MZ interferometer sequence shown in Fig. 1 with the initial conditions $r_{0j}(t_i) = z_i\delta_{jz}$ and $\dot{r}_{0j}(t_i) = 0$, we therefore find

$$\begin{aligned} f_\phi &= 31g^2v_rT^6/20 - v_r gT^4(14z_i + 9v_rT)/4 \\ &\quad + v_rT^2(v_r^2T^2 + 3v_rTz_i + 3z_i^2), \end{aligned} \quad (\text{E3})$$

$$f_{rr} = v_rT^2, \quad f_{rp} = v_rT^3, \quad f_{pp} = \frac{7}{6}v_rT^4. \quad (\text{E4})$$

-
- [1] M. Kasevich and S. Chu, Atomic Interferometry Using Stimulated Raman Transitions, *Phys. Rev. Lett.* **67**, 181 (1991).
- [2] A. Peters, K. Y. Chung, and S. Chu, Measurement of gravitational acceleration by dropping atoms, *Nature (London)* **400**, 849 (1999).
- [3] T. Farah, C. Guerlin, A. Landragin, P. Bouyer, S. Gaffet, F. Pereira Dos Santos, and S. Merlet, Underground operation at best sensitivity of the mobile LNE-SYRTE cold atom gravimeter, *Gyroscopy Navig.* **5**, 266 (2014).
- [4] M. J. Snadden, J. M. McGuirk, P. Bouyer, K. G. Haritos, and M. A. Kasevich, Measurement of the Earth's Gravity Gradient with an Atom Interferometer-Based Gravity Gradiometer, *Phys. Rev. Lett.* **81**, 971 (1998).
- [5] G. W. Biedermann, X. Wu, L. Deslauriers, S. Roy, C. Mahadeswaraswamy, and M. A. Kasevich, Testing gravity with cold-atom interferometers, *Phys. Rev. A* **91**, 033629 (2015).
- [6] P. Asenbaum, C. Overstreet, T. Kovachy, D. D. Brown, J. M. Hogan, and M. A. Kasevich, Phase Shift in an Atom Interferometer Due to Spacetime Curvature Across Its Wave Function, *Phys. Rev. Lett.* **118**, 183602 (2017).
- [7] S. Fray, C. A. Diez, T. W. Hänsch, and M. Weitz, Atomic Interferometer with Amplitude Gratings of Light and Its Applications to Atom Based Tests of the Equivalence Principle, *Phys. Rev. Lett.* **93**, 240404 (2004).
- [8] D. Schlippert, J. Hartwig, H. Albers, L. L. Richardson, C. Schubert, A. Roura, W. P. Schleich, W. Ertmer, and E. M. Rasel, Quantum Test of the Universality of Free Fall, *Phys. Rev. Lett.* **112**, 203002 (2014).
- [9] M. G. Tarallo, T. Mazzoni, N. Poli, D. V. Sutyryn, X. Zhang, and G. M. Tino, Test of Einstein Equivalence Principle for 0-Spin and Half-Integer-Spin Atoms: Search for Spin-Gravity Coupling Effects, *Phys. Rev. Lett.* **113**, 023005 (2014).
- [10] L. Zhou, S. Long, B. Tang, X. Chen, F. Gao, W. Peng, W. Duan, J. Zhong, Z. Xiong, J. Wang *et al.*, Test of Equivalence Principle at 10^{-8} Level by a Dual-Species Double-Diffraction Raman Atom Interferometer, *Phys. Rev. Lett.* **115**, 013004 (2015).

- [11] A. Wicht, J. M. Hensley, E. Sarajlic, and S. Chu, A preliminary measurement of the fine structure constant based on atom interferometry, *Phys. Scr.* **T102**, 82 (2002).
- [12] R. H. Parker, C. Yu, W. Zhong, B. Estey, and H. Müller, Measurement of the fine-structure constant as a test of the Standard Model, *Science* **360**, 191 (2018).
- [13] P. W. Graham, J. M. Hogan, M. A. Kasevich, and S. Rajendran, Resonant mode for gravitational wave detectors based on atom interferometry, *Phys. Rev. D* **94**, 104022 (2016).
- [14] M. Sonnleitner, M. Ritsch-Marte, and H. Ritsch, Attractive Optical Forces from Blackbody Radiation, *Phys. Rev. Lett.* **111**, 023601 (2013).
- [15] P. Haslinger, M. Jaffe, V. Xu, O. Schwartz, M. Sonnleitner, M. Ritsch-Marte, H. Ritsch, and H. Müller, Attractive force on atoms due to blackbody radiation, *Nat. Phys.* **14**, 257 (2018).
- [16] P. Storey and C. Cohen-Tannoudji, The Feynman path integral approach to atomic interferometry. A tutorial, *J. Phys. II France* **4**, 1999 (1994).
- [17] C. Antoine and C. J. Bordé, Exact phase shifts for atom interferometry, *Phys. Lett. A* **306**, 277 (2003).
- [18] B. Dubetsky, S. Libby, and P. Berman, Atom interferometry in the presence of an external test mass, *Atoms* **4**, 14 (2016).
- [19] E. Giese, S. Kleinert, M. Meister, V. Tamma, A. Roura, and W. P. Schleich, The interface of gravity and quantum mechanics illuminated by Wigner phase space, in *Proceedings of the International School of Physics “Enrico Fermi”*, Course 188 *Atom Interferometry*, edited by G. M. Tino and M. A. Kasevich (IOS Press, Amsterdam, 2014), p. 171.
- [20] W. P. Schleich, D. M. Greenberger, and E. M. Rasel, A representation-free description of the Kasevich-Chu interferometer: A resolution of the redshift controversy, *New J. Phys.* **15**, 013007 (2013).
- [21] K.-P. Marzlin and J. Audretsch, State independence in atom interferometry and insensitivity to acceleration and rotation, *Phys. Rev. A* **53**, 312 (1996).
- [22] S. Kleinert, E. Kajari, A. Roura, and W. P. Schleich, Representation-free description of light-pulse atom interferometry including non-inertial effects, *Phys. Rep.* **605**, 1 (2015).
- [23] J. M. Hogan, D. M. S. Johnson, and M. A. Kasevich, Light-pulse atom interferometry, in *Proceedings of the International School of Physics “Enrico Fermi”*, Course 168, *Atom Optics and Space Physics*, edited by E. Arimondo, W. Ertmer, W. P. Schleich, and E. M. Rasel (OS Press, Amsterdam, 2009), p. 411.
- [24] A. Roura, W. Zeller, and W. P. Schleich, Overcoming loss of contrast in atom interferometry due to gravity gradients, *New J. Phys.* **16**, 123012 (2014).
- [25] W. Zeller, The impact of wave-packet dynamics in long-time atom interferometry, Ph.D. thesis, Universität Ulm, 2016.
- [26] W. Magnus, On the exponential solution of differential equations for a linear operator, *Commun. Pure Appl. Math* **7**, 649 (1954).
- [27] S. Blanes, F. Casas, J. A. Oteo, and J. Ros, A pedagogical approach to the Magnus expansion, *Eur. J. Phys.* **31**, 907 (2010).
- [28] C. Ufrecht, Theoretical approach to high-precision atom interferometry, Ph.D. thesis, Universität Ulm, 2019.
- [29] H. Ribeiro, A. Baksic, and A. A. Clerk, Systematic Magnus-Based Approach for Suppressing Leakage and Nonadiabatic Errors in Quantum Dynamics, *Phys. Rev. X* **7**, 011021 (2017).
- [30] H. Cramér, *Mathematical Methods of Statistics* (Princeton University Press, Princeton, NJ, 1999).
- [31] E. Wodey, D. Tell, E. M. Rasel, D. Schlippert, R. Baur, U. Kissling, B. Kölliker, M. Lorenz, M. Marrer, U. Schlöpfer *et al.*, A scalable high-performance magnetic shield for very long baseline atom interferometry, *Rev. Sci. Instrum.* **91**, 035117 (2020).
- [32] C. Ufrecht, F. Di Pumpo, A. Friedrich, A. Roura, C. Schubert, D. Schlippert, E. M. Rasel, W. P. Schleich, and E. Giese, An atom interferometer testing the universality of free fall and the gravitational redshift, [arXiv:2001.09754](https://arxiv.org/abs/2001.09754) (2020).
- [33] A. Bertoldi, F. Minardi, and M. Prevedelli, Phase shift in atom interferometers: Corrections for nonquadratic potentials and finite-duration laser pulses, *Phys. Rev. A* **99**, 033619 (2019).
- [34] S. Loriani, A. Friedrich, C. Ufrecht, F. Di Pumpo, S. Kleinert, S. Abend, N. Gaaloul, C. Meiners, C. Schubert, D. Tell *et al.*, Interference of clocks: A quantum twin paradox, *Sci. Adv.* **5**, eaax8966 (2019).
- [35] C. Chiu and L. Stodolsky, Theorem in matter-wave interferometry, *Phys. Rev. D* **22**, 1337 (1980).
- [36] D. M. Greenberger, The neutron interferometer as a device for illustrating the strange behavior of quantum systems, *Rev. Mod. Phys.* **55**, 875 (1983).
- [37] M. Sanz, E. Solano, and Í. L. Egusquiza, Beyond adiabatic elimination: Effective Hamiltonians and singular perturbation, in *Applications + Practical Conceptualization+ Mathematics= Fruitful Innovation* (Springer, Tokyo, 2016).
- [38] E. Giese, A. Roura, G. Tackmann, E. M. Rasel, and W. P. Schleich, Double Bragg diffraction: A tool for atom optics, *Phys. Rev. A* **88**, 053608 (2013).
- [39] L. V. Keldysh, Diagram technique for nonequilibrium processes, *J. Exp. Theor. Phys.* **20**, 1018 (1965).
- [40] J. Schwinger, Brownian motion of a quantum oscillator, *J. Math. Phys.* **2**, 407 (1961).
- [41] A. Peters, K. Y. Chung, and S. Chu, High-precision gravity measurements using atom interferometry, *Metrologia* **38**, 25 (2001).
- [42] C. J. Bordé, Theoretical tools for atom optics and interferometry, *C. R. Acad. Sci.* **2**, 509 (2001).
- [43] A. Roura, Circumventing Heisenberg’s Uncertainty Principle in Atom Interferometry Tests of the Equivalence Principle, *Phys. Rev. Lett.* **118**, 160401 (2017).
- [44] H. Ammann and N. Christensen, Delta Kick Cooling: A New Method for Cooling Atoms, *Phys. Rev. Lett.* **78**, 2088 (1997).
- [45] R. Kubo, Generalized cumulant expansion method, *J. Phys. Soc. Jpn.* **17**, 1100 (1962).
- [46] P. R. Halmos, *Measure theory*, Graduate Texts in Mathematics (Springer, New York, 2014).
- [47] W. Schleich, *Quantum Optics in Phase Space* (Wiley, Berlin, 2001).
- [48] W. B. Case, Wigner functions and Weyl transforms for pedestrians, *Am. J. Phys.* **76**, 937 (2008).